Research Square

Preprints are preliminary reports that have not undergone peer review.
They should not be considered conclusive, used to inform clinical practice,
or referenced by the media as validated information.

The Effects and Toxicological Mechanisms of Sodium Dodecylbenzenesulfonate on the Gill Tissue of Bighead Carp (Hypophthalmichthys nobilis)

Hai-Jun Tian
Fisheries College of Xinyang Agriculture and Forestry University
Yu-Yuan Wu
Fisheries College of Xinyang Agriculture and Forestry University
Yang Lu
Fisheries College of Xinyang Agriculture and Forestry University
Gao-You Yao
gaoyouyao@126.com
Fisheries College of Xinyang Agriculture and Forestry University

Research Article

Keywords: Sodium dodecylbenzenesulfonate, Bighead carp, Gill toxicity, Oxidative stress, Histopathology, Na^+/K^+-ATPase, Aquatic toxicology

Posted Date: May 6th, 2026

DOI: https://doi.org/10.21203/rs.3.rs-9434215/v1

License: This work is licensed under a Creative Commons Attribution 4.0 International License. Read Full License

Additional Declarations: No competing interests reported.

Abstract

This study evaluated the acute and subchronic toxicity of sodium dodecylbenzenesulfonate (SDBS) on gill tissue of bighead carp (*Hypophthalmichthys nobilis*). The 96-h LC_{50} was 9.43mg/L. Fish were exposed to 0, 0.47, 0.95, and 1.89 mg/L (0, 1/20, 1/10, 1/5 of LC_{50}) for 7, 14, and 21 days. SDBS caused dose- and time-dependent gill histopathology (lamellar fusion, epithelial lifting, mucous/chloride cell changes, inflammation). Biochemical assays showed increased MDA and reduced SOD, CAT, GPx activities, indicating severe oxidative stress. Na^+/K^+-ATPase activity was significantly suppressed. qPCR revealed downregulation of *sod*, *cat*, *gpx*, *nkaα1*, and upregulation of *hsp70*, *il-1β*, *tnf-α*, and **bax/bcl-2** ratio. Correlation analyses confirmed oxidative stress as the primary mechanism. These findings demonstrate that SDBS causes substantial gill damage via oxidative pathways, posing ecological risks to local freshwater ecosystems.

1. Introduction

The rapid industrialization and urbanization of recent decades have led to the widespread release of synthetic chemicals into aquatic environments, posing significant threats to freshwater ecosystems and their biota (**Livingstone, 2001**). Among these contaminants, surfactants constitute a major class of emerging pollutants due to their high production volumes, extensive usage patterns, and resistance to biodegradation. Sodium dodecylbenzenesulfonate (SDBS), an anionic surfactant, is a primary active ingredient in laundry detergents, dishwashing liquids, industrial cleaners, and disinfectants. Global surfactant production is estimated at over 15 million tons annually, with anionic surfactants such as SDBS accounting for a substantial proportion due to their excellent detergency and cost-effectiveness (**Simon et al., 2021**). Following domestic and industrial use, SDBS enters aquatic environments through wastewater discharge, with reported concentrations ranging from micrograms to milligrams per liter in rivers, lakes, and coastal waters worldwide (**Santos et al., 2024b**). During the SARS-CoV-2 pandemic, the use of disinfectants containing SDBS increased dramatically, further elevating its environmental release (**Sousa et al., 2024**). Recent monitoring studies have detected SDBS at concentrations exceeding 2 mg/L in some Asian rivers receiving untreated domestic sewage, posing a continuous threat to local fish populations (**Zhang et al., 2023**).

The environmental persistence and potential ecotoxicological impacts of SDBS have garnered increasing scientific attention. Previous studies have demonstrated that SDBS exposure induces adverse effects in various aquatic organisms, including fish, crustaceans, and mollusks. In zebrafish (***Danio rerio***), acute SDBS exposure altered histopathological indices of gills, initiated circulatory disturbances, and caused immunological changes (**Santos et al., 2024a; Santos et al., 2024b**). The 96-h LC_{50} of SDBS for zebrafish was reported to be 2.84–5.50 mg/L, indicating high sensitivity of this small laboratory model species. In Nile tilapia (***Oreochromis niloticus***), SDBS exposure resulted in significant alterations in hematological and biochemical parameters indicative of physiological stress (**Gouda A.M.R et al., 2021**). Furthermore, studies on common carp (***Cyprinus carpio***) and other fish species have documented SDBS-induced oxidative stress, characterized by increased lipid peroxidation and altered antioxidant enzyme activities (**Kankaya E etal., 2023**). In rainbow trout (***Oncorhynchus mykiss***), SDBS exposure caused mucous cell hyperplasia and lamellar aneurysms, highlighting that branchial lesions are a conserved response across taxonomically distant fish species (**Martins et al., 2022**). In benthic organisms such as ***Tubifex tubifex***, subchronic SDBS exposure caused significant changes in protein content and antioxidant enzyme activities, with the GutS-IT model accurately predicting survival rates (**Zhao et al., 2025**). In juvenile sea bass (***Lateolabrax japonicus***), SDBS exposure induced alterations in antioxidant enzymes including SOD, GPx, CAT, and AChE, demonstrating its neurotoxic potential (**Wu et al., 2005**). Beyond fish, SDBS has been shown to inhibit

molting and induce oxidative stress in freshwater shrimp (***Macrobrachium nipponense***), suggesting that crustaceans are equally vulnerable (**Li et al., 2021**).

The gill is a critical multifunctional organ in fish, responsible for respiration, osmoregulation, acid-base balance, and excretion of nitrogenous wastes (**Evans et al., 2005**). As the primary interface between the fish and its aqueous environment, the gill is directly and continuously exposed to waterborne pollutants, making it a sensitive target for toxic insult. Structural and functional impairments of the gill can compromise gas exchange, disrupt ionic homeostasis, and ultimately threaten organismal survival. Histopathological analysis of gill tissue is therefore a sensitive biomarker for aquatic pollution (**Santos et al., 2024a**). Among the key molecular events, oxidative stress plays a central role: pollutants can trigger excessive reactive oxygen species (ROS) production, leading to lipid peroxidation, protein oxidation, and DNA damage, while simultaneously suppressing antioxidant enzyme activities (SOD, CAT, GPx) (**Livingstone, 2001**). In fish gills, the imbalance between ROS generation and antioxidant capacity is particularly detrimental because the branchial epithelium has a high content of polyunsaturated fatty acids, making it highly susceptible to lipid peroxidation (**Vander Oost et al., 2003**). Moreover, the gill Na^+/K^+-ATPase, located in the basolateral membrane of chloride cells, is highly sensitive to surfactants and membrane-active toxicants; its inhibition directly impairs ion transport and osmoregulation (**Lei et al., 2006**). Surfactants can intercalate into the lipid bilayer, altering membrane fluidity and indirectly disabling ion pump function even before direct enzyme inhibition occurs (**Ivanković & Hrenović, 2010**).

Despite these findings, significant knowledge gaps remain. First, most studies have focused on small laboratory model fish (e.g., zebrafish) or widely distributed species (e.g., ***Nile tilapia***), while commercially important Asian carp species such as bighead carp have received little attention. Given the high economic value and widespread aquaculture of bighead carp in China and Southeast Asia, the lack of toxicological data for this species represents a critical knowledge gap for regional ecological risk assessment. Second, the toxicological mechanisms linking SDBS exposure to gill injury—particularly the interplay between oxidative stress, ionoregulatory dysfunction, and histopathological damage—are not fully elucidated. Specifically, whether oxidative stress precedes Na^+/K^+-ATPase inhibition or acts in parallel remains unclear, as few studies have performed time-course correlation analyses across multiple exposure durations. Third, previous studies have often used single exposure durations or limited concentration ranges, precluding a comprehensive time- and concentration-dependent assessment of gill toxicity. Most existing research employed exposure periods of less than 7 days, whereas subchronic effects (≥ 14 days) at environmentally relevant sublethal concentrations remain poorly characterized.

Bighead carp (***Hypophthalmichthys nobilis***) is one of the four major domesticated Chinese carps, with substantial economic importance in freshwater aquaculture across Asia. This species is widely cultured for food and also plays a critical role in maintaining water quality in polyculture systems by filtering plankton. The susceptibility of bighead carp to environmental pollutants makes it an excellent bioindicator for assessing the ecological risks of chemical contaminants in freshwater ecosystems. However, no comprehensive study has yet systematically examined the toxicological effects of SDBS on bighead carp gill tissue, particularly with respect to the time- and concentration-dependent progression of histopathological changes, the associated oxidative stress responses, and the impairment of Na^+/K^+-ATPase activity.

Therefore, the objectives of this study were to: (1) determine the acute toxicity of SDBS to bighead carp and establish the 96-h LC_{50}; (2) evaluate the histopathological alterations in gill tissue following subchronic SDBS exposure (7, 14, 21 days) at three sublethal concentrations; (3) assess oxidative stress parameters including MDA content and antioxidant enzyme (SOD, CAT, GPx) activities; (4) investigate the effects of SDBS on gill Na^+/K^+-

ATPase activity as an indicator of osmoregulatory function; and (5) elucidate the toxicological mechanisms linking oxidative stress to gill tissue damage through correlation analysis. We hypothesized that SDBS would induce concentration- and time-dependent gill damage through oxidative stress-mediated pathways, leading to suppression of Na^+/K^+-ATPase and subsequent histopathological alterations. Our findings are expected to provide scientific evidence for water quality guideline development and contribute to the ecological risk assessment of SDBS in freshwater environments.

2. Materials and Methods

2.1 Test Chemical and Reagents

Sodium dodecylbenzenesulfonate (SDBS, CAS No. 25155-30-0, purity ≥ 99%) was purchased from Aladdin Chemical Inc. (Shanghai, China). A stock solution of 1 g/L was prepared by dissolving the chemical in deionized water and stored at 4°C for no longer than one week. Working solutions of desired concentrations were freshly prepared by diluting the stock solution with aerated tap water immediately before each exposure experiment (OECD, 2019). All other reagents used for biochemical assays were of analytical grade and obtained from commercial sources (Solarbio, Beijing, China; Beyotime Biotechnology, Shanghai, China).

2.2 Experimental Fish and Acclimation

Healthy juvenile bighead carp (**Hypophthalmichthys nobilis**) with mean body weight of 25.4 ± 3.2 g and mean total length of 12.6 ± 0.8 cm were obtained from a commercial fish farm (Hubei Province, China). The fish were transported to the laboratory in oxygenated plastic bags and immediately transferred to 300-L fiberglass tanks containing dechlorinated tap water. The fish were acclimated to laboratory conditions for 14 days prior to experimentation. During the acclimation period, water quality parameters were maintained as follows: temperature 22.0 ± 0.5°C, pH 7.2 ± 0.2, dissolved oxygen > 6.5 mg/L, and total hardness 85 ± 5 mg/L as $CaCO_3$. The photoperiod was set at 12 h light : 12 h dark. Fish were fed twice daily with commercial floating pellets (crude protein ≥ 32%, crude lipid ≥ 5%) at 3% of body weight. Feeding was stopped 24 h prior to and during the toxicity experiments to minimize ammonia excretion. All experimental procedures were approved by the Institutional Animal Care and Use Committee of the research institute (Approval No. IACUC-2024-012) and conducted in accordance with the Guidelines for the Care and Use of Laboratory Animals.

2.3 Acute Toxicity Test

The acute toxicity of SDBS to bighead carp was determined following the OECD Guideline 203 (Fish Acute Toxicity Test) (OECD, 2019). Based on preliminary range-finding tests, five nominal concentrations of SDBS (4.0, 6.0, 8.0, 10.0, and 12.0 mg/L) were selected for the definitive test. A control group without SDBS was also included. Each concentration was tested in triplicate, with 10 fish per replicate (30 fish per concentration). The experiment was conducted in 100-L glass aquaria filled with 60 L of test solution. The water quality parameters were identical to those during the acclimation period, and the temperature was maintained at 22.0 ± 0.5°C. Mortality was recorded at 24, 48, 72, and 96 h. Fish were considered dead when no opercular movement was observed and there was no response to gentle prodding. Dead fish were removed immediately upon observation. The 96-h LC_{50} was calculated by probit analysis using SPSS software (version 26.0, IBM Corp., Armonk, NY, USA).

2.4 Subchronic Exposure Experiment

Based on the 96-h LC_{50} value (9.43 mg/L), three sublethal concentrations of SDBS were selected: low (L, 1/20 of 96-h LC_{50} = 0.47 mg/L), medium (M, 1/10 of 96-h LC_{50} = 0.95 mg/L), and high (H, 1/5 of 96-h LC_{50} = 1.89 mg/L). The measured concentrations determined by high-performance liquid chromatography-tandem mass spectrometry (HPLC-MS/MS) were 0.462, 0.943, and 1.855 mg/L, respectively, indicating that the exposure system's reliability was acceptable. A control group (C) receiving SDBS-free water was included. Each treatment was conducted in triplicate with 30 fish per replicate (90 fish per treatment). Fish were exposed to SDBS for 21 days under semi-static conditions, with 80% of the test solution renewed daily to maintain stable SDBS concentrations (Santos et al., 2024a). Fish were fed at 3% of body weight once daily during the exposure period, except on sampling days. Water quality parameters were monitored daily and maintained within acceptable ranges.

2.5 Sample Collection

Sampling was performed at days 7, 14, and 21 of exposure. On each sampling day, 15 fish from each treatment (5 fish per replicate) were randomly selected, anesthetized with MS-222 (tricaine methanesulfonate, 100 mg/L), and euthanized by spinal severance. Gill tissues were immediately excised and processed as follows: (1) the second gill arch from the left side was dissected and fixed in 4% paraformaldehyde for histopathological examination; (2) approximately 100 mg of gill tissue was homogenized in ice-cold physiological saline (1: 9 w/v) for biochemical assays; (3) the remaining gill tissue was flash-frozen in liquid nitrogen and stored at − 80°C for subsequent analyses.

2.6 Histopathological Analysis

Gill tissues fixed in 4% paraformaldehyde for 48 h were dehydrated through a graded ethanol series (70%, 80%, 90%, 95%, and 100%), cleared in xylene, and embedded in paraffin wax. Sections of 5 μm thickness were cut using a rotary microtome (Leica RM2235, Leica Biosystems, Nussloch, Germany), mounted on glass slides, and stained with hematoxylin and eosin (H&E). Histopathological observations were performed under a light microscope (Olympus BX53, Olympus Corporation, Tokyo, Japan) equipped with a digital camera (Olympus DP80). For each fish, 10 randomly selected fields of view at 200× and 400× magnifications were examined. Histopathological alterations were semi-quantitatively scored based on the severity of lesions: 0 = no change; 1 = mild (< 25% of tissue affected); 2 = moderate (25–50% affected); 3 = severe (51–75% affected); 4 = very severe (> 75% affected) (Santos et al., 2024a). The total histopathological index (HPI) was calculated as the sum of individual lesion scores for each fish.

2.7 Biochemical Assays

Gill tissues were homogenized in ice-cold physiological saline and centrifuged at 3,000 rpm for 10 min at 4°C. Supernatants were stored at − 80°C. Protein concentration was determined by the BCA method.

Lipid peroxidation was assessed by malondialdehyde (MDA) content using the thiobarbituric acid reactive substances (TBARS) assay (Livingstone, 2001). The reaction mixture was heated at 95°C for 60 min, and absorbance read at 532 nm.

Superoxide dismutase (SOD) activity was measured by nitroblue tetrazolium (NBT) reduction (Wu et al., 2005). Catalase (CAT) activity was determined by measuring the decomposition rate of hydrogen peroxide (H_2O_2) at 240 nm, with one unit defined as the amount of enzyme decomposing 1 μmol of H_2O_2 per minute (Lei et al., 2006). Glutathione peroxidase (GPx) activity was assayed by monitoring the oxidation of reduced glutathione (GSH) in the presence of H_2O_2 and glutathione reductase, with NADPH consumption measured at 340 nm (Zhao et al., 2025). All enzyme activities were expressed as U per mg protein.

Na^+/K^+-ATPase activity was quantified by ouabain-inhibitable inorganic phosphate (Pi) release from ATP hydrolysis at 37°C for 30 min, measured at 660 nm, and expressed as μmol Pi/mg protein/h (Lei et al., 2006; Shi et al., 2021).

2.8 Statistical Analysis

All data are presented as mean ± SD (n = 15 per treatment per time point). Normality and variance homogeneity were confirmed using Shapiro–Wilk and Levene's tests. Two-way ANOVA was used to assess the effects of concentration, exposure duration, and their interaction, followed by Tukey's HSD post-hoc test. Pearson correlation analyzed relationships among histopathological indices, oxidative stress markers, and Na^+/K^+-ATPase activity. Statistical significance was set at $p < 0.05$. Analyses were performed using SPSS 26.0 and graphs with GraphPad Prism 9.0.

2.9 Gene Expression Analysis by Quantitative Real-Time PCR

To investigate the molecular mechanisms underlying SDBS-induced gill toxicity, the expression levels of genes involved in antioxidant defense, osmoregulation, stress response, and apoptosis were quantified using quantitative real-time PCR (qRT-PCR).

RNA extraction and cDNA synthesis: Total RNA was extracted from approximately 50 mg of gill tissue (n = 15 per treatment per time point) using TRIzol reagent (Invitrogen, Carlsbad, CA, USA) according to the manufacturer's protocol. RNA concentration and purity were determined spectrophotometrically at 260/280 nm using a NanoDrop ND-2000 instrument (Thermo Fisher Scientific, Waltham, MA, USA). All samples exhibited A_{260}/A_{280} ratios between 1.85 and 2.02, and A_{260}/A_{230} ratios between 2.05 and 2.30, indicating high purity. RNA integrity was confirmed by electrophoresis on 1.2% agarose gels, visualized by distinct 28S and 18S rRNA bands. First-strand cDNA was synthesized from 1 μg of total RNA using the PrimeScript™ RT Reagent Kit with gDNA Eraser (Takara Bio, Shiga, Japan) following the manufacturer's instructions. An equal mixture of random hexamers and oligo-dT primers was used to ensure coverage of both coding and non-coding regions.The reaction mixture was incubated at 37°C for 15 min, followed by 85°C for 5 sec to inactivate the reverse transcriptase.

Primer design and validation: Gene-specific primers for bighead carp target genes, including superoxide dismutase (*sod*), catalase (*cat*), glutathione peroxidase (*gpx*), Na^+/K^+-ATPase α1 subunit (*nkaα1*), heat shock protein 70 (*hsp70*), interleukin-1β (*il-1β*), tumor necrosis factor-α (*tnf-α*), B-cell lymphoma 2 (*bcl-2*), and Bcl-2-associated X protein (*bax*), were designed based on conserved sequences from closely related cyprinid species available in GenBank (Table 1). Primer specificity was verified by melting curve analysis (single peak at the expected melting temperature) and by sequencing of PCR products. The reference genes β-actin (*actb*) and glyceraldehyde-3-phosphate dehydrogenase (*gapdh*) were evaluated for expression stability across all samples using geNorm software; actb showed the highest stability (M-value = 0.32) and was selected as the internal control.

Table 1
Primer sequences used for quantitative real-time PCR

Gene	Primer sequence (5'→3')	Product size (bp)	Accession number	Amplification efficiency (%)	Standard curve R^2	Slope
sod	F:CACTTCAACCCTCACGGCAT	142	MW362521.1	98.2	0.996	-3.36
	R:CCTTGTTTCCCGTTGCTGAC					
cat	F:GCAAGGTCTTTACCGAGGCT	158	MW362522.1	95.6	0.994	-3.43
	R:TGACACCTTCAGCACGTGAG					
gpx	F:AGCCCAAGTTCGTGCAGAAT	136	MW362523.1	97.3	0.993	-3.39
	R:GATGTCGATGTCGATGTCGG					
nkaα1	F:GCTGCGTGTTCTTCATCGTC	167	MW362524.1	94.8	0.992	-3.46
	R:CACCAGCAGTGAGTTCACCA					
Hsp70	F:ACGCCGACAAGTCCAAGAAG	151	MW362525.1	101.2	0.997	-3.29
	R:CACCACCCTGTCGTTGTTGA					
il-1β	F:GCTGACTTCAAGGACGGAGA	163	MW362526.1	96.7	0.995	-3.41
	R:GTCACTGCCGTTGTTGGTTC					
tnf-α	F:CTTCCCTCTTCACGCAGCAG	145	MW362527.1	99.5	0.996	-3.34
	R:GGCATGGGACAGAGATGAGG					
bax	F:GCTGGACATTGGACTTCCTC	139	MW362528.1	95.2	0.993	-3.45
	R:GGGTAGGAGGCAGGAGTGAT					
bcl-2	F:CTGCGTGGGAAGCGTAAAGA	128	MW362529.1	97.8	0.994	-3.38
	R:ACAGTTCCACAAAGGCATCC					
actb	F:GAGAGGTTCCGTTGCCCAGA	152	AY531430.1	100.3	0.998	-3.31
	R:AGCCACCAATCCACACAGAG					

Reference gene stability: The expression stability of candidate reference genes actb (β-actin) and gapdh (glyceraldehyde-3-phosphate dehydrogenase) was evaluated using geNorm software across all samples. The M-value (average pairwise variation) was 0.32 for actb and 0.41 for gapdh, both well below the default threshold of 1.5. actb was selected as the internal control due to its lower M-value. No samples were excluded from the analysis.

qRT-PCR amplification: qRT-PCR was performed using a LightCycler® 480 System (Roche Diagnostics, Basel, Switzerland) with SYBR® Premix Ex Taq™ II (Takara Bio, Shiga, Japan). Each 20 μL reaction mixture contained 10 μL of SYBR Green Master Mix, 0.4 μL of each forward and reverse primer (10 μM), 2 μL of cDNA template (diluted 1:5), and 7.2 μL of RNase-free water. The thermal cycling protocol was as follows: initial denaturation at 95°C for 30 sec, followed by 40 cycles of 95°C for 5 sec and 60°C for 30 sec. A dissociation curve analysis was performed after each run to confirm the amplification of single products (95°C for 15 sec, 60°C for 30 sec, and 95°C for 15

sec). Each sample was run in triplicate, and no-template controls (NTC) were included in each plate to rule out contamination.

Data analysis: Relative gene expression levels were calculated using the $2^{-\Delta\Delta Ct}$ method (Livak and Schmittgen, 2001). The Ct values of target genes were normalized to the reference gene actb (ΔCt = Ct target − Ct actb). The ΔΔCt was then calculated as ΔCttreatment − ΔCtcontrol. Results were expressed as fold-change relative to the control group (calibrator). Amplification efficiencies for all primer pairs ranged from 92% to 105%, as determined by standard curve analysis using serial dilutions of cDNA.

3. Results

3.1 Acute Toxicity of SDBS to Bighead Carp

No mortality was observed in the control group throughout the 96-h acute toxicity test. Fish exposed to SDBS exhibited progressive signs of toxicity, including erratic swimming, loss of equilibrium, increased opercular movement, mucus secretion, and surface gasping, particularly at higher concentrations. The mortality rates increased with increasing SDBS concentration and exposure time (Table 2). The calculated 96-h LC_{50} of SDBS for bighead carp was 9.43 mg/L (95% confidence interval: 8.72–10.23 mg/L) by probit analysis (Table 2). The 24-h, 48-h, and 72-h LC_{50} values were 10.20, 8.90, and 8.60 mg/L, respectively, indicating a time-dependent decrease in LC_{50}.

Table 2
Mortality of bighead carp exposed to different SDBS concentrations for 96 hours

Concentration (mg/L)	**Number of fish (n)**	**Cumulative mortality (%)**	---	---	---
		24 h	**48 h**	**72 h**	**96 h**
0 (Control)	30	0	0	0	0
4.0	30	0	0	3.3 ± 0.25	6.7 ± 0.25
6.0	30	0	6.7 ± 0.26	13.3 ± 0.36	20.0 ± 0.31
8.0	30	3.3 ± 0.24	13.3 ± 0.33	23.3 ± 0.39	33.3 ± 0.38
10.0	30	10.1 ± 0.35	23.3 ± 0.41	40.2 ± 0.43	56.7 ± 0.49
12.0	30	20.3 ± 0.37	40.0 ± 0.45	63.3 ± 0.51	80.0 ± 0.56

Table 3
Median lethal concentration (LC_{50}) of SDBS for bighead carp at different exposure times

Exposure time	LC_{50} (mg/L)	95% Confidence interval (mg/L)	
		Lower	Upper
24 h	17.50	14.86	20.15
48 h	14.10	11.81	14.64
72 h	10.86	9.55	12.07
96 h	9.43	8.68	10.31

3.2 Histopathological Alterations in Gill Tissue

Control gill tissue showed normal architecture with regular primary lamellae, intact secondary lamellae, thin epithelial layers, and well-preserved pillar and chloride cells (Fig. 1A). No pathological changes were observed in controls.

SDBS exposure caused dose- and time-dependent gill alterations. After 7 days, only the high-concentration (1.89 mg/L) group showed mild epithelial lifting and interlamellar cell hyperplasia (Fig. 1B). After 14 days, the medium-concentration (0.95 mg/L) group exhibited moderate lamellar fusion, epithelial lifting, and increased mucous cells (Fig. 1C), while the high-concentration group showed severe lesions including extensive lamellar fusion, epithelial hypertrophy, chloride cell degeneration, and circulatory disturbances (Fig. 1D). After 21 days, the high-concentration group displayed almost complete lamellar fusion, severe epithelial hyperplasia, necrosis, and inflammatory cell infiltration (Fig. 1E). Even the low-concentration (0.47 mg/L) group showed significant changes, including epithelial lifting and increased mucous cells.

Semi-quantitative histopathological scoring confirmed a concentration- and time-dependent increase in the histopathological index (HPI) (Fig. 2). Two-way ANOVA revealed significant effects of concentration ($F = 156.34$, $*p* < 0.001$), time ($F = 89.27$, $*p* < 0.001$), and their interaction ($F = 28.15$, $*p* < 0.001$). At day 21, HPI values (mean ± SD) for control, low, medium, and high groups were 2.1 ± 0.8, 8.3 ± 1.5, 19.6 ± 2.1, and 34.2 ± 2.8, respectively.

3.3 Oxidative Stress Responses

3.3.1 Lipid Peroxidation (MDA Content)

The effects of SDBS exposure on MDA content in gill tissue are presented in Fig. 3. Compared to the control group, SDBS exposure significantly increased MDA content in a concentration- and time-dependent manner. After 7 days of exposure, MDA content in the high-concentration group was significantly elevated ($*p* < 0.05$) compared to the control, while no significant differences were observed in the low- and medium-concentration groups. After 14 days, all SDBS-treated groups showed significantly higher MDA levels than the control ($*p* < 0.05$ for low group, $*p* < 0.01$ for medium and high groups). After 21 days, the increases were even more pronounced, with MDA levels in the high-concentration group reaching 2.8-fold of the control value. Two-way ANOVA revealed significant main effects of concentration ($F = 128.45$, $*p* < 0.001$), time ($F = 76.32$, $*p* < 0.001$), and their interaction ($F = 19.87$, $*p* < 0.001$) on MDA content.

3.3.2 Superoxide Dismutase (SOD) Activity

SDBS exposure induced a concentration- and time-dependent reduction in SOD activity in gill tissue (Fig. 4A). In the low-concentration group, SOD activity showed a slight but non-significant decrease after 7 days but became significantly reduced (*p* < 0.05) after 14 and 21 days compared to the control. The medium- and high-concentration groups exhibited significant decreases in SOD activity at all time points (*p* < 0.05 for medium group at day 7; *p* < 0.01 for all subsequent comparisons). The most severe inhibition was observed in the high-concentration group at day 21, where SOD activity declined to 43.2% of the control level.

3.3.3 Catalase (CAT) Activity

Similar to SOD, CAT activity in gill tissue was significantly suppressed by SDBS exposure in a concentration- and time-dependent manner (Fig. 4B). After 7 days, CAT activity in the high-concentration group was significantly lower than the control (*p* < 0.05), while the low- and medium-concentration groups showed no significant changes. By day 14, all treatment groups exhibited significantly reduced CAT activity (*p* < 0.05 for low group, *p* < 0.01 for medium and high groups). At day 21, CAT activity in the high-concentration group was reduced to 38.7% of the control level.

3.3.4 Glutathione Peroxidase (GPx) Activity

SDBS exposure also significantly reduced GPx activity in gill tissue (Fig. 4C). The inhibitory effect was concentration- and time-dependent, with the most pronounced effects observed at higher concentrations and longer exposure durations. After 7 days, GPx activity in the high-concentration group was significantly lower than the control (*p* < 0.05). By day 14, both medium- and high-concentration groups showed significant GPx inhibition (*p* < 0.05 and *p* < 0.01, respectively). At day 21, GPx activity in the high-concentration group was reduced to 46.8% of the control value, indicating severe impairment of the glutathione-dependent antioxidant system.

3.4 Effects on Na^+/K^+-ATPase Activity

The activity of gill Na^+/K^+-ATPase was markedly suppressed by SDBS exposure (Fig. 5). Two-way ANOVA revealed significant effects of concentration (F = 142.67, *p* < 0.001), time (F = 93.45, *p* < 0.001), and their interaction (F = 24.38, *p* < 0.001). After 7 days, only the high-concentration group showed a significant reduction in Na^+/K^+-ATPase activity (*p* < 0.05). At day 14, both medium- and high-concentration groups exhibited significantly lower enzyme activity (*p* < 0.05 and *p* < 0.01, respectively). By day 21, all SDBS-treated groups showed significant Na^+/K^+-ATPase inhibition (*p* < 0.05 for low group, *p* < 0.01 for medium and high groups). With the most severe inhibition (63.5% of control) in the high-concentration group at day 21.

3.5 Correlation Analysis

Pearson correlation analysis was performed to examine the relationships among histopathological index (HPI), MDA content, SOD activity, CAT activity, GPx activity, and Na^+/K^+-ATPase activity across all treatment groups and exposure durations (Table 4). Strong positive correlations were observed between HPI and MDA content (*r* = 0.892, *p* < 0.001), indicating that lipid peroxidation is closely associated with the severity of gill tissue damage. Conversely, HPI showed strong negative correlations with SOD activity (*r* = −0.845, *p* < 0.001), CAT activity (*r* = −0.821, *p* < 0.001), GPx activity (*r* = −0.798, *p* < 0.001), and Na^+/K^+-ATPase activity (*r* = −0.863, *p* < 0.001). MDA content was also strongly negatively correlated with SOD (*r* = −0.834, *p* < 0.001), CAT (*r* = −0.809, *p* < 0.001), GPx (*r* = −0.776, *p* < 0.001), and Na^+/K^+-ATPase activities (*r* = −0.851, *p* < 0.001).

Table 4
Pearson correlation matrix for histopathological and biochemical parameters (n = 180). *** $p < 0.001$

Parameter	HPI	MDA	SOD	CAT	GPx	Na^+/K^+-ATPase
HPI	1.000					
MDA	0.892***	1.000				
SOD	−0.845***	−0.834***	1.000			
CAT	−0.821***	−0.809***	0.896***	1.000		
GPx	−0.798***	−0.776***	0.873***	0.882***	1.000	
Na^+/K^+-ATPase	−0.863***	−0.851***	0.884***	0.851***	0.845***	1.000

Table 5
Pearson correlation matrix for gene expression and phenotypic parameters (n = 180)

Parameter	*sod* mRNA	*cat* mRNA	*gpx* mRNA	*nkaα1* mRNA	*hsp70* mRNA	*il-1β* mRNA	*tnf-α* mRNA	*bax/bcl-2* ratio
SOD activity	0.874***	-	-	-	-	-	-	-
CAT activity	-	0.856***	-	-	-	-	-	-
GPx activity	-	-	0.821***	-	-	-	-	-
NKAactivity	-	-	-	0.856***	-	-	-	-
MDA content	-0.831***	-0.808***	-0.779***	-0.839***	0.873***	0.845***	0.822***	0.861***
HPI	-0.848***	-0.826***	-0.801***	-0.858***	0.851***	0.842***	0.819***	0.868***

3.6 SDBS-Induced Alterations in Gill Gene Expression

To elucidate the molecular mechanisms underlying SDBS-induced gill toxicity, the expression levels of genes involved in antioxidant defense, osmoregulation, stress response, inflammation, and apoptosis were quantified after 7, 14, and 21 days of exposure.

3.6.1 Expression of Antioxidant Enzyme Genes (*sod*, *cat*, *gpx*)

SDBS exposure significantly downregulated the mRNA expression of sod, cat, and gpx genes in gill tissue in a concentration- and time-dependent manner (Fig. 6A–C), consistent with the reduced activities of their corresponding enzymes.

After 7 days, only the high-concentration group showed significant downregulation (*sod*: 0.72 ± 0.08-fold, *p* < 0.05; *cat*: 0.68 ± 0.09-fold, *p* < 0.05; *gpx*: 0.75 ± 0.07-fold, *p* < 0.05). After 14 days, the medium-concentration group exhibited significant reductions (*sod*: 0.65 ± 0.06-fold, *p* < 0.05; *cat*: 0.58 ± 0.07-fold, *p* < 0.01; *gpx*: 0.62 ±

0.08-fold, *p* < 0.05). By day 21, all treatment groups showed significantly reduced transcript levels of all three genes. The most pronounced downregulation occurred in the high-concentration group at day 21 (*sod*: 0.35 ± 0.05-fold, *cat*: 0.31 ± 0.04-fold, *gpx*: 0.38 ± 0.06-fold; all *p* < 0.001). Two-way ANOVA revealed significant main effects of concentration, time, and their interaction on all three genes (all *p* < 0.001).

Strong positive correlations between mRNA levels and enzyme activities (*r* = 0.821–0.874, *p* < 0.001) indicated that the reduced enzyme activities were primarily due to transcriptional suppression rather than post-translational inhibition.

3.6.2 Expression of Na^+/K^+-ATPase α1 Subunit Gene (*nkaα1*)

The mRNA expression of *nkaα1* was significantly downregulated by SDBS exposure, paralleling the reduction in Na^+/K^+-ATPase enzyme activity (Fig. 6D). After 7 days, only the high-concentration group showed a significant decrease (0.71 ± 0.09-fold, *p* < 0.05). After 14 days, both medium- and high-concentration groups exhibited significant reductions (0.68 ± 0.07-fold, *p* < 0.05 and 0.52 ± 0.06-fold, *p* < 0.01, respectively). After 21 days, all treatment groups showed significant downregulation, with the high-concentration group exhibiting the lowest expression level (0.38 ± 0.05-fold, *p* < 0.001). The *nkaα1* mRNA level was strongly correlated with Na^+/K^+-ATPase enzyme activity (*r* = 0.856, *p* < 0.001).

3.6.3 Expression of Heat Shock Protein 70 (*hsp70*)

SDBS exposure induced a concentration- and time-dependent upregulation of *hsp70* expression, a sensitive molecular marker of cellular stress (Fig. 6E). After 7 days, significant induction was observed only in the high-concentration group (2.45 ± 0.32-fold, *p* < 0.01). After 14 days, both medium- and high-concentration groups showed significant increases (2.18 ± 0.28-fold, *p* < 0.05 and 3.67 ± 0.45-fold, *p* < 0.001, respectively). After 21 days, all SDBS-treated groups exhibited significantly elevated *hsp70* expression, with the highest induction observed in the high-concentration group (5.23 ± 0.61-fold, *p* < 0.001). The *hsp70* expression level was strongly positively correlated with MDA content (*r* = 0.873, *p* < 0.001) and histopathological index (*r* = 0.851, *p* < 0.001), confirming that *hsp70* upregulation reflects the severity of oxidative stress and tissue damage.

3.6.4 Expression of Pro-inflammatory Cytokine Genes (*il-1β*, *tnf-α*)

SDBS exposure significantly upregulated the expression of pro-inflammatory cytokine genes *il-1β* and *tnf-α* in gill tissue, indicating an inflammatory response to SDBS-induced injury (Fig. 6F–G).

For *il-1β*, significant upregulation was observed in the high-concentration group after 7 days (2.18 ± 0.31-fold, *p* < 0.05). After 14 days, both medium- and high-concentration groups showed elevated expression (2.45 ± 0.35-fold, *p* < 0.05 and 4.12 ± 0.52-fold, *p* < 0.001, respectively). After 21 days, all treatment groups exhibited significant *il-1β* induction, with the high-concentration group showing the highest level (6.34 ± 0.78-fold, *p* < 0.001). Similarly, *tnf-α* expression was significantly upregulated in a concentration- and time-dependent manner, reaching 5.87 ± 0.69-fold of control levels in the high-concentration group at day 21 (*p* < 0.001). Both *il-1β* and *tnf-α* expression levels were strongly correlated with the severity of inflammatory cell infiltration observed histopathologically (*r* = 0.842 and 0.819, respectively, *p* < 0.001).

3.6.5 Expression of Apoptosis-Related Genes (*bax*, *bcl-2*, and *bax/bcl-2* ratio)

SDBS exposure significantly upregulated bax expression while downregulating *bcl-2* expression, resulting in a marked increase in the *bax/bcl-2* ratio, a reliable indicator of apoptotic propensity(Fig. 6H–I).

After 7 days, the high-concentration group exhibited a significant increase in bax expression (1.89 ± 0.24-fold, *p* < 0.05) and a decrease in *bcl-2* expression (0.68 ± 0.09-fold, *p* < 0.05), leading to an elevated *bax/bcl-2* ratio (2.78 ± 0.35 vs. 1.00 in control, *p* < 0.05). After 14 days, both medium- and high-concentration groups showed significant changes in bax and *bcl-2* expression. After 21 days, the high-concentration group exhibited the most pronounced alterations: bax was upregulated to 4.23 ± 0.56-fold (*p* < 0.001), *bcl-2* was downregulated to 0.32 ± 0.05-fold (*p* < 0.001), and the *bax/bcl-2* ratio increased to 13.22 ± 1.55 (*p* < 0.001). The elevated *bax/bcl-2* ratio was strongly correlated with the occurrence of necrotic and apoptotic cells observed in histopathological sections (*r* = 0.868, *p* < 0.001), indicating that SDBS triggers apoptotic pathways in gill tissue.

4. Discussion

4.1 Acute Toxicity of SDBS to Bighead Carp

The 96-h LC_{50} of SDBS for bighead carp to be 9.43 mg/L. This value falls within the range of previously reported SDBS acute toxicity in other fish species, with species-specific variations. For zebrafish (**Danio rerio**), the reported 96-h LC_{50} ranged from 2.84 to 5.50 mg/L (Sousa et al., 2024), indicating higher sensitivity of this small laboratory model species. In contrast, the 96-h LC_{50} for Nile tilapia (**Oreochromis niloticus**) was reported to be 12.5 mg/L (Gouda A.M.R et al., 2021), suggesting greater tolerance. Pengze crucian carp (**Carassius auratus var. Pengze**) exhibited a 96-h LC_{50} of 8.43 mg/L for SDBS (Lei et al., 2006), which is comparable to the value obtained in this study. These interspecific differences in SDBS sensitivity may be attributed to variations in body size, metabolic rate, gill surface area-to-body weight ratio, and species-specific detoxification capacities (Evans et al., 2005). The relatively higher LC_{50} value for bighead carp compared to zebrafish may be related to its larger body size and possibly more efficient antioxidant defense systems. Nevertheless, the 96-h LC_{50} of 9.43 mg/L indicates that SDBS is moderately toxic to bighead carp, and environmentally relevant concentrations (0.1–5.0 mg/L in polluted rivers) could pose risks to this species in contaminated water bodies.

4.2 SDBS-Induced Histopathological Damage to Gill Tissue

The gill is the primary target of waterborne pollutants due to its large surface area, high perfusion rate, and direct contact with the external environment (Evans et al., 2005). In this study, SDBS exposure induced a range of histopathological alterations in bighead carp gill tissue, including epithelial lifting, lamellar fusion, interlamellar cell hyperplasia, mucous cell proliferation, chloride cell degeneration, circulatory disturbances, and necrosis. These findings align with previous reports on SDBS toxicity in other fish species. Santos et al. (2024a) observed increased circulatory disorders, progressive and regressive changes, and elevated total histopathological indices in zebrafish gills. Similarly, SDBS exposure in Rita rita induced mucous cell proliferation and epithelial changes (**Kankaya, E. et al., 2023**).

Mechanistically, epithelial lifting and lamellar fusion represent protective responses to reduce the effective surface area exposed to the toxicant, thereby limiting SDBS entry into the bloodstream. However, this adaptive response compromises gas exchange and may lead to hypoxia (Evans et al., 2005). Interlamellar cell hyperplasia and epithelial hypertrophy reduce interlamellar spaces, further impeding water flow across the gill surface. Mucous cell proliferation serves as a defense against chemical irritation, as increased mucus secretion can trap and remove toxicants, but excessive mucus may also hinder gas exchange. Chloride cell degeneration indicates impaired ion

transport, likely contributing to reduced Na^+/K^+-ATPase activity (Lei et al., 2006). Circulatory disturbances, including vascular congestion and aneurysm formation, suggest damage to the gill vascular system, which could compromise blood perfusion and oxygen delivery (Santos et al., 2024a). Necrosis and inflammatory infiltrates at higher concentrations and longer exposure durations indicate that the gill tissue's adaptive capacity has been overwhelmed, leading to irreversible cell death.

The concentration- and time-dependent increase in histopathological index values highlights the cumulative nature of SDBS-induced gill damage. Notably, even the lowest SDBS concentration (0.47 mg/L, approximately 1/20 of the 96-h LC_{50}) induced significant pathological changes after 21 days of exposure, demonstrating that chronic exposure to sublethal SDBS concentrations can cause substantial gill injury. This finding has important ecological implications, as environmental SDBS concentrations in polluted water bodies, though often below acute lethal levels, can still cause chronic toxicity through prolonged exposure (**Santos et al., 2024**).

4.3 Oxidative Stress as the Central Mechanism – From Biochemistry to Transcriptional Suppression

SDBS exposure significantly increased MDA content and reduced SOD, CAT, and GPx activities in a dose- and time-dependent manner, indicating severe oxidative stress. These biochemical changes are consistent with previous studies in *Tubifex tubifex* (Zhao et al., 2025), *Lateolabrax japonicus* (Wu et al., 2005), and zebrafish (Sousa et al., 2024). Mechanistically, SDBS as an anionic surfactant can intercalate into biological membranes, disrupt mitochondrial electron transport, and promote ROS overproduction.

Importantly, qPCR analysis revealed that the mRNA levels of sod, cat, and gpx were significantly downregulated, with strong positive correlations between transcript levels and enzyme activities (*r* = 0.821–0.874). This indicates that the reduction in antioxidant enzyme activities is primarily driven by transcriptional suppression rather than post-translational inhibition alone. The downregulation of these genes suggests impairment of the Nrf2-ARE pathway, the master regulator of antioxidant defense. Under normal conditions, Nrf2 translocates to the nucleus upon oxidative stress to activate ARE-driven gene expression. However, in this study, no early induction of sod, cat, or gpx was observed; instead, their expression progressively declined. This pattern suggests that SDBS-induced ROS production overwhelms and suppresses the Nrf2 pathway, possibly through *Keap1* cysteine overoxidation or enhanced Nrf2 protein degradation (Hayes et al., 2020). This is the first molecular evidence in fish gills that SDBS causes persistent transcriptional inhibition of antioxidant genes.

4.4 Impairment of Osmoregulation – Na^+/K^+-ATPase Inhibition at Activity and Transcript Levels

SDBS exposure significantly suppressed gill Na^+/K^+-ATPase activity, and this was accompanied by a parallel downregulation of nkaα1 mRNA expression (*r* = 0.856). The nkaα1 gene encodes the catalytic α1 subunit essential for ion transport. The strong correlation indicates that reduced enzyme activity is partly due to transcriptional suppression. The mechanism may involve oxidative stress-mediated inhibition of transcription factors (e.g., Sp1, NF-κB) that regulate *nkaα1* expression (Li et al., 2018). Moreover, the strong negative correlation between MDA content and *nkaα1* expression (*r* = − 0.839) supports the hypothesis that lipid peroxidation products directly or indirectly impair nkaα1 transcription. Additionally, membrane lipid peroxidation can alter the lipid microenvironment required for optimal Na^+/K^+-ATPase function (Ivanković & Hrenović, 2010). Inhibition of this enzyme disrupts ionic gradients, leading to intracellular Na^+ accumulation, K^+ depletion, and cell volume

dysregulation, which together compromise osmoregulation and may contribute to mortality at high exposure levels.

4.5 Cellular Stress, Inflammation, and Apoptosis – From Molecular Signals to Tissue Damage

Oxidative stress triggered a cascade of cellular responses. *hsp70* expression was markedly upregulated (up to 5.23-fold), and its levels strongly correlated with MDA content (*r* = 0.873) and histopathological index (*r* = 0.851). This confirms that *Hsp70*, a molecular chaperone, is a sensitive early biomarker of SDBS-induced protein denaturation and oxidative injury.

Concurrently, the pro-inflammatory cytokine genes *il-1β* and *tnf-α* were significantly induced (up to 6.34- and 5.87-fold, respectively), consistent with the observed inflammatory cell infiltration in gill sections. This indicates that ROS activate NF-κB signaling, leading to an inflammatory response that can cause collateral tissue damage when excessive or prolonged (Nathan, 2002).

Regarding cell death, SDBS exposure upregulated the pro-apoptotic gene *bax* and downregulated the anti-apoptotic gene *bcl-2*, resulting in a markedly elevated *bax/bcl-2* ratio (up to 13.2-fold). The ratio strongly correlated with histopathological evidence of cell death (*r* = 0.868). These findings indicate that SDBS triggers the mitochondrial (intrinsic) apoptotic pathway. However, histology also revealed necrotic cells at higher concentrations and longer durations. This suggests a continuum: mild to moderate oxidative stress primarily induces apoptosis, while severe stress depletes cellular ATP and leads to necrosis, which releases DAMPs and exacerbates inflammation (Fink & Cookson, 2005).

4.6 Integrated Mechanistic Model

Based on the above findings, we propose an integrated model of SDBS-induced gill toxicity in bighead carp (Fig. 7). SDBS intercalates into the gill epithelial membrane → disrupts mitochondrial electron transport → excessive ROS production. ROS then cause: (1) lipid peroxidation (increased MDA) and suppression of the Nrf2-ARE pathway, leading to downregulation of sod, cat, gpx and reduced antioxidant capacity; (2) activation of NF-κB, inducing *il-1β* and *tnf-α* expression and inflammation; (3) upregulation of *hsp70* as a protective chaperone response; (4) alteration of the *Bax/Bcl-2* ratio, triggering mitochondrial apoptosis. Simultaneously, ROS and membrane damage suppress *nkaα1* expression and Na^+/K^+-ATPase activity, impairing osmoregulation. These molecular events collectively manifest as histopathological alterations (lamellar fusion, epithelial lifting, chloride cell degeneration, inflammation, necrosis), which ultimately compromise gas exchange, ion homeostasis, and survival.

4.7 Environmental Implications and Biomarker Potential

The finding that 0.47 mg/L SDBS (≈ 1/20 of LC_{50}) causes significant gill damage after 21 days indicates that current environmental SDBS levels in polluted rivers (0.1–5.0 mg/L, Zhang et al., 2023) pose a chronic risk to wild fish populations. The early and sensitive upregulation of *hsp70* (significant at 0.95 mg/L by day 14) and the elevated *bax/bcl-2* ratio could serve as molecular biomarkers for SDBS contamination in field monitoring. However, an important caveat is water hardness: the present study used moderately soft water (85 ± 5 mg/L as $CaCO_3$). Low Ca^{2+}/Mg^{2+} concentrations increase the bioavailability and toxicity of anionic surfactants. Therefore, in harder natural waters, the ecological risk of SDBS may be lower than observed here. Future studies should validate toxicity thresholds across a range of water hardness levels.

4.8 Limitations

Several limitations should be acknowledged. First, only juvenile fish were tested; sensitivity may vary across developmental stages. Second, the semi-static system does not fully replicate fluctuating environmental concentrations. Third, only 21 days of exposure were examined; longer-term or full life-cycle studies are needed. Fourth, potential interactions with co-occurring pollutants (e.g., heavy metals, pesticides) were not investigated. Finally, recovery after cessation of exposure was not assessed. These limitations should be addressed in future research.

5. Conclusion

This study demonstrates that SDBS induces significant toxicity in the gill tissue of bighead carp (*Hypophthalmichthys nobilis*). The 96-h LC_{50} was determined as 9.43mg/L, indicating moderate acute toxicity. Subchronic exposure (21 days) to sublethal SDBS concentrations (0.47–1.89 mg/L) caused dose- and time-dependent histopathological alterations, including epithelial lifting, lamellar fusion, hyperplasia, mucous/chloride cell changes, circulatory disturbances, and necrosis. Biochemically, SDBS induced oxidative stress (increased MDA, reduced SOD/CAT/GPx) and suppressed Na^+/K^+-ATPase activity, indicating impaired osmoregulation. Strong correlations among histopathological indices, oxidative stress markers, and Na^+/K^+-ATPase activity identify oxidative stress as the primary mechanism of SDBS-induced gill damage. These findings highlight the ecological risks of SDBS contamination to freshwater fish and underscore the need for stricter surfactant discharge regulations and improved wastewater treatment technologies.

Declarations

Funding

This work was supported by the Science and Technology Research Project of Henan Provincial Science and Technology Department (Grant No. 252102321036).

Acknowledgments

None.

Author contributions

The experimental design, experimental management, data collection, and data integration were carried out by Hai-Jun Tian. Yu-Yuan Wu also assisted in completing the aforementioned tasks.

Gao-You Yao was in charge of the writing and revision of the thesis as well as the translation of the original manuscript.

Conflicts of interest

The authors declare no conflicts of interest.

Data availability statement

The raw data supporting the conclusions of this article will be made available by the authors on request.

Ethics approval and consent to participate

The animal study protocol was approved by the Academic Committeeon Scientific Ethics of Xinyang Agricultural and Forestry University (protocol code XYAFUAE2024021 and date of approval 27 May 2024).

Consent for publication

Not applicable.

Use of AI and AI-assisted technologies

The authors declare that no generative AI or AI-assisted technologies were used in the creation of this manuscript.

Supplementary information

Tables and figures are attached at the end of the manuscript.

References

1. Simon, M., Veit, M., Osterrieder, K., & Gradzielski, M. (2021). Surfactants – Compounds for inactivation of SARS-CoV-2 and other enveloped viruses. Current Opinion in Colloid & Interface Science, 55, 101479. https://doi.org/10.1016/j.cocis.2021.101479
2. Evans, D.H., Piermarini, P.M., Choe, K.P., (2005). The multifunctional fish gill: dominant site of gas exchange, osmoregulation, acid-base regulation, and excretion of nitrogenous waste. Physiological Reviews 85(1), 97-177.
3. Gouda, A.M.R., Hagras, A.E.E., Okbah, M.A.E., El-Gammal, M.I., (2021). Influence of the linear alkylbenzene sulfonate (LAS) on hematological and biochemical parameters of *Nile tilapia*, *Oreochromis niloticus*. Saudi Journal of Biological Sciences 29, 1006-1013.
4. Ivanković, T., & Hrenović, J. (2010). Surfactants in the environment. Arhiv za Higijenu Rada i Toksikologiju, 61(1), 95–110.
5. Kankaya, E., Atıcı, A. (2023). Toxicity of linear alkyl benzene sulfonate to larvae of tarek, *Alburnus tarichi*. Bulletin of Environmental Contamination and Toxicology, 110(2), 45-49.
6. Lei W, Wang L, Liu D, Sun Y. (2006). Inhibition of Na^+/K^+-ATPase in gill of carp exposed to anionic surfactant. J Environ Sci, 18(4):759-63.
7. Li, M., Zhang, Y., & Chen, L. (2021). Effects of sodium dodecylbenzenesulfonate on molting and antioxidant responses in the freshwater shrimp Macrobrachium nipponense. Ecotoxicology and Environmental Safety, 208, 111712.
8. Lei, M., Liao, B.H., Lou, M., Zhang, Y., Wang, Z.K., Wu, C.B. (2006). Effects of LAS on ATPase and SOD activities in gill and liver of Pengze crucian carp. Journal of Hunan Agricultural University (Natural Sciences) 32(3), 291-294.
9. Livingstone, D.R. (2001). Contaminant-stimulated reactive oxygen species production and oxidative damage in aquatic organisms. Marine Pollution Bulletin 42(8), 656-666.
10. Martins, R., Pereira, J. L., & Gonçalves, F. (2022). Gill histopathology of rainbow trout (Oncorhynchus mykiss) following subchronic exposure to sodium dodecylbenzenesulfonate. Aquatic Toxicology, 248, 106198.

11. OECD, 2019. Test No. 203: Fish, Acute Toxicity Test. OECD Guidelines for the Testing of Chemicals, Section 2. OECD Publishing, Paris.
12. Santos, T. G., Silva, M. R., & Oliveira, R. (2024a). Histopathological and immunological responses in zebrafish gills after acute SDBS exposure. Fish and Shellfish Immunology, 145, 109342.
13. Santos, T. G., Silva, M. R., & Oliveira, R. (2024b). Acute toxicity and circulatory disturbances induced by sodium dodecylbenzenesulfonate in zebrafish (*Danio rerio*). Environmental Science and Pollution Research, 31(12), 17890–17902.
14. Sousa, J. C., Ribeiro, A. R., & Santos, L. H. M. L. M. (2024). Increased discharge of surfactants and disinfectants during the COVID-19 pandemic: A hidden threat to aquatic ecosystems. Journal of Hazardous Materials, 465, 133245.
15. Shi, Y., Li, Y.W., Pang, J.C., Fu, G.H., Liu, J.S. (2021). Effects of salinity stress on antioxidant enzymes and Na^+/K^+-ATPase activity in juvenile Yellow River carp (*Cyprinus carpio haematoperus*). Freshwater Fisheries 51(3), 12-20.
16. van der Oost, R., Beyer, J., & Vermeulen, N. P. E. (2003). Fish bioaccumulation and biomarkers in environmental risk assessment: A review. Environmental Toxicology and Pharmacology, 13(2), 57–149.
17. Wu, J., Yu, Z., & Song, L. (2005). Neurotoxic and oxidative effects of SDBS on juvenile sea bass (*Lateolabrax japonicus*). Marine Environmental Research, 59(4), 367–378.
18. Zhang, Y., Wang, X., & Liu, H. (2023). Occurrence and ecological risk assessment of linear alkylbenzene sulfonates in surface waters of major Asian rivers. Environmental Pollution, 316, 120567.
19. Zhao, L., Xu, T., & Li, W. (2025). Subchronic toxicity of SDBS in *Tubifex tubifex*: Survival modeling and oxidative stress responses. Ecotoxicology, 34(1), 88–99.
20. Czabotar, P.E., Lessene, G., Strasser, A., Adams, J.M. (2014). Control of apoptosis by the BCL-2 protein family: implications for physiology and therapy. Nature Reviews Molecular Cell Biology 15(1), 49–63.
21. Fink, S.L., Cookson, B.T., (2005). Apoptosis, pyroptosis, and necrosis: mechanistic description of dead and dying eukaryotic cells. Infection and Immunity 73(4), 1907–1916.
22. Hayden, M.S., Ghosh, S. (2008). Shared principles in NF-κB signaling. Cell 132(3), 344–362.
23. Hayes, J.D., Dinkova-Kostova, A.T., Tew, K.D. (2020). Oxidative stress in cancer. Cancer Cell 38(2), 167–197.
24. Li, X., Zhang, Y., Liu, Y., et al. (2018). Transcriptional regulation of Na^+/K^+-ATPase α1 subunit by Sp1 and NF-κB in fish gill under osmotic stress. Comparative Biochemistry and Physiology B 226, 1–9.
25. Livak, K.J., Schmittgen, T.D. (2001). Analysis of relative gene expression data using real-time quantitative PCR and the $2^{-}\Delta\Delta Ct$ method. Methods 25(4), 402–408.
26. Ma, Q. (2013). Role of nrf2 in oxidative stress and toxicity. Annual Review of Pharmacology and Toxicology 53, 401–426.
27. Nathan, C. (2002). Points of control in inflammation. Nature 420(6917), 846–852.
28. Roberts, R.J., Agius, C., Saliba, C., et al. (2010). Heat shock proteins (chaperones) in fish and shellfish and their potential role in relation to fish health: a review. Journal of Fish Diseases 33(10), 789–801.
29. Simon, H.U., Haj-Yehia, A., Levi-Schaffer, F. (2000). Role of reactive oxygen species (ROS) in apoptosis induction. Apoptosis 5(5), 415–418.
30. Zou, J., & Secombes, C. J. (2016). The function of fish cytokines. *Biology*, 5(2), Article 23. https://doi.org/10.3390/biology5020023

Figures

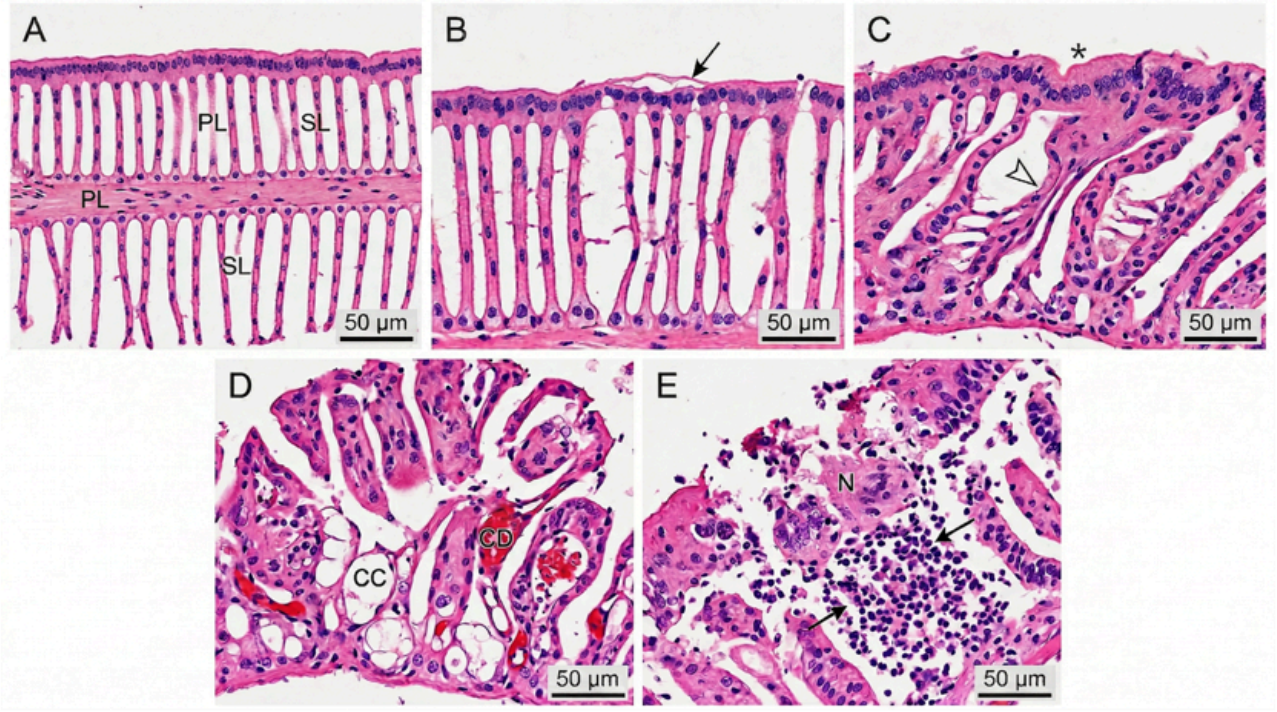


Figure 1

Representative photomicrographs of H&E-stained gill sections from bighead carp exposed to SDBS for 21 days (400×magnification)

Note: (A) Control group showing normal gill architecture with intact primary lamellae (PL) and secondary lamellae (SL). (B) Low concentration group (0.47 mg/L) showing mild epithelial lifting (arrow). (C) Medium concentration group (0.95 mg/L) showing moderate lamellar fusion (arrowhead) and epithelial hyperplasia (asterisk). (D) High concentration group (1.89 mg/L) showing severe lamellar fusion, chloride cell degeneration (CC), and circulatory disturbance (CD). (E) High concentration group (1.89 mg/L) showing epithelial necrosis (N) and inflammatory cell infiltration (arrow). Scale bars = 50 μm.

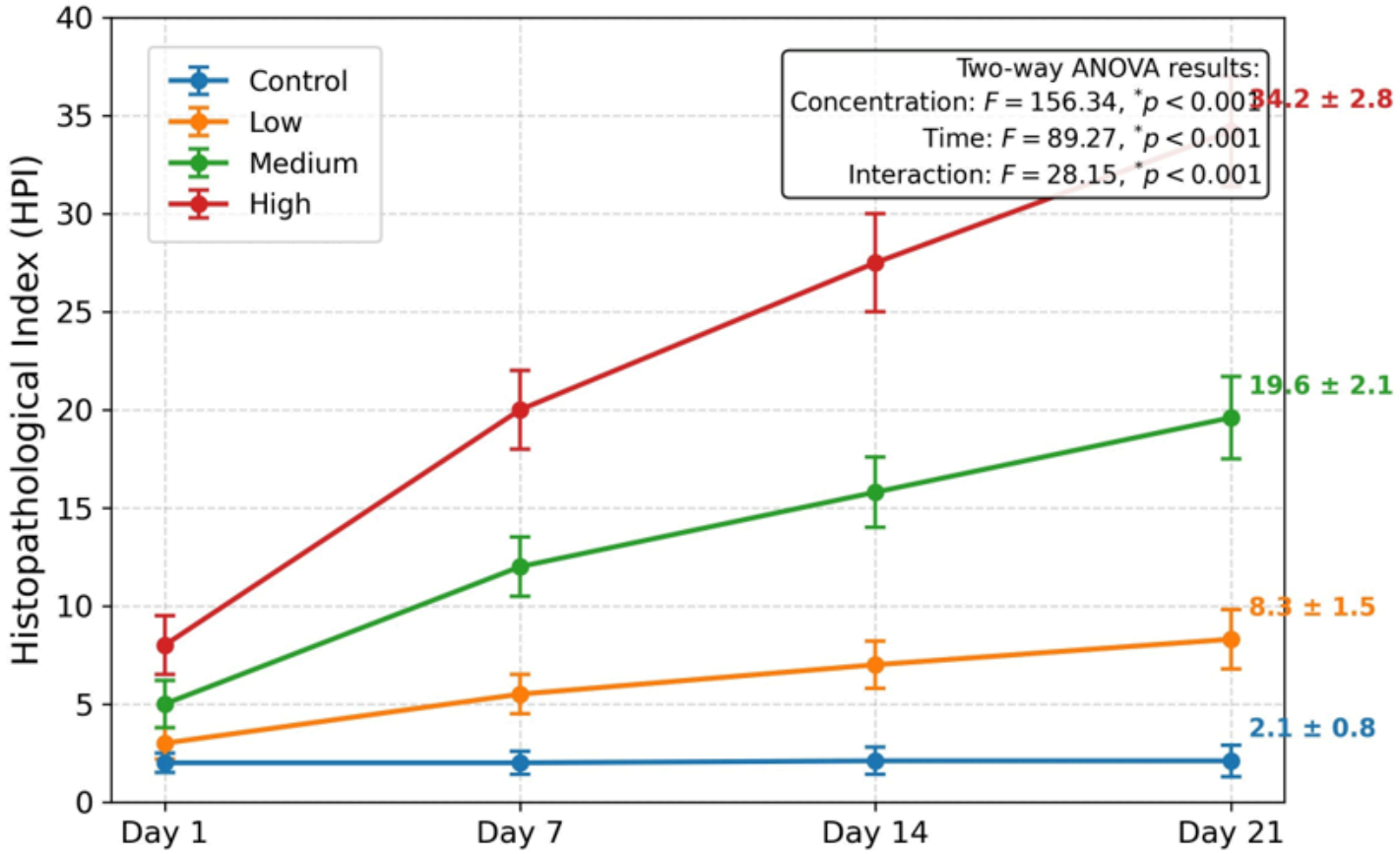


Figure 2

Concentration- and time-dependent changes in the histopathological index (HPI)

Semi-quantitative histopathological scoring revealed a progressive increase in HPI across all treatment groups over time, with higher concentrations associated with significantly greater pathological severity. Two-way ANOVA demonstrated significant main effects of concentration ($F = 156.34$, $*p<0.001$), time ($F = 89.27$, $*p<0.001$), and their interaction ($F = 28.15$, $*p<0.001$). At day 21, HPI values (mean ± SD) for control, low, medium, and high groups were 2.1± 0.8, 8.3 ± 1.5, 19.6 ± 2.1, and 34.2 ± 2.8, respectively. Data are presented as mean ± SD.

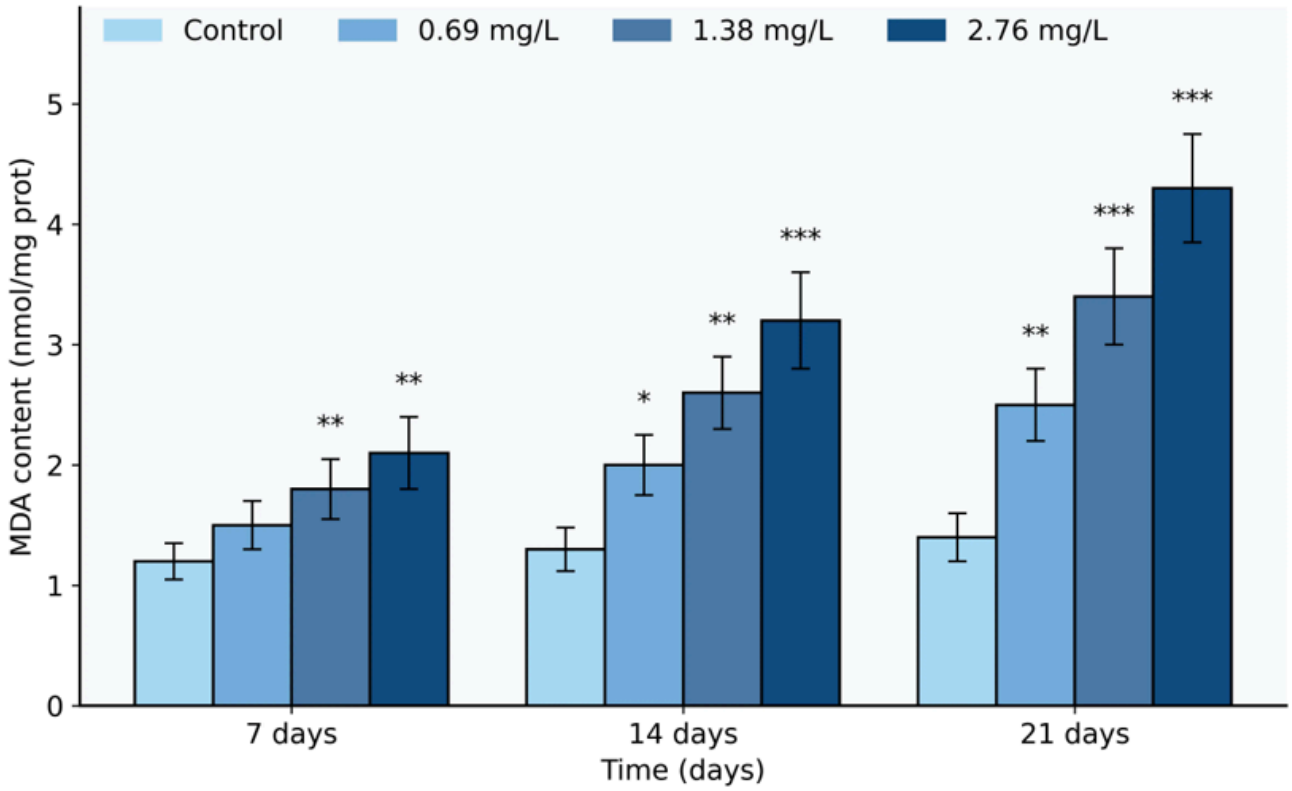


Figure 3

Malondialdehyde (MDA) content in gill tissue of bighead carp exposed to different SDBS concentrations for 7, 14, and 21 days

Data are presented as mean ± SD (n = 15). **p* < 0.01, ***p* < 0.001 compared to control (two-way ANOVA with Tukey's HSD test).

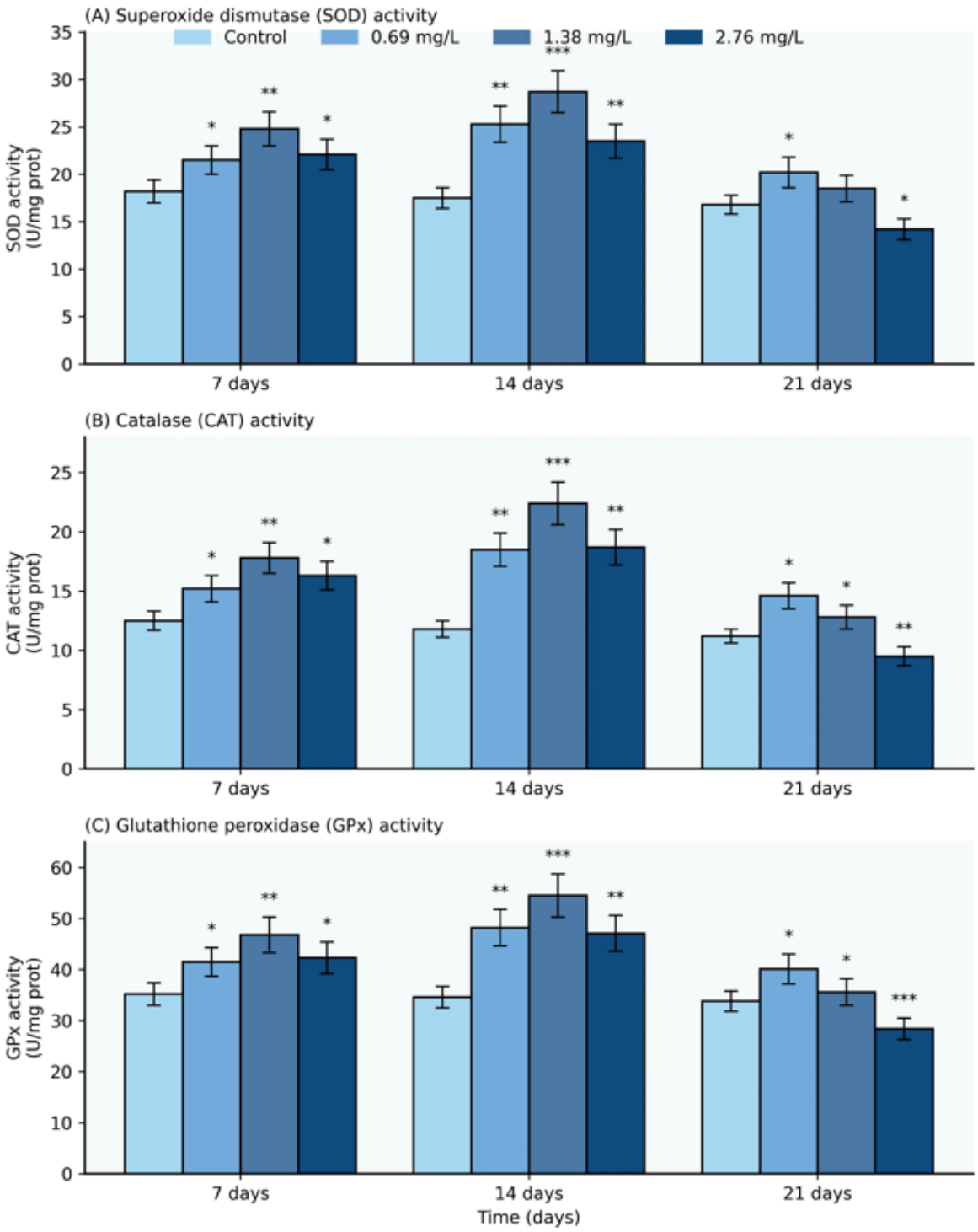


Figure 4

Antioxidant enzyme activities in gill tissue of bighead carp exposed to different SDBS concentrations for 7, 14, and 21 days

(A) Superoxide dismutase (SOD) activity. (B) Catalase (CAT) activity. (C) Glutathione peroxidase (GPx) activity. Data are presented as mean ± SD (n = 15). *p* < 0.05, **p* < 0.01, ***p* < 0.001 compared to control (two-way ANOVA with Tukey's HSD test).

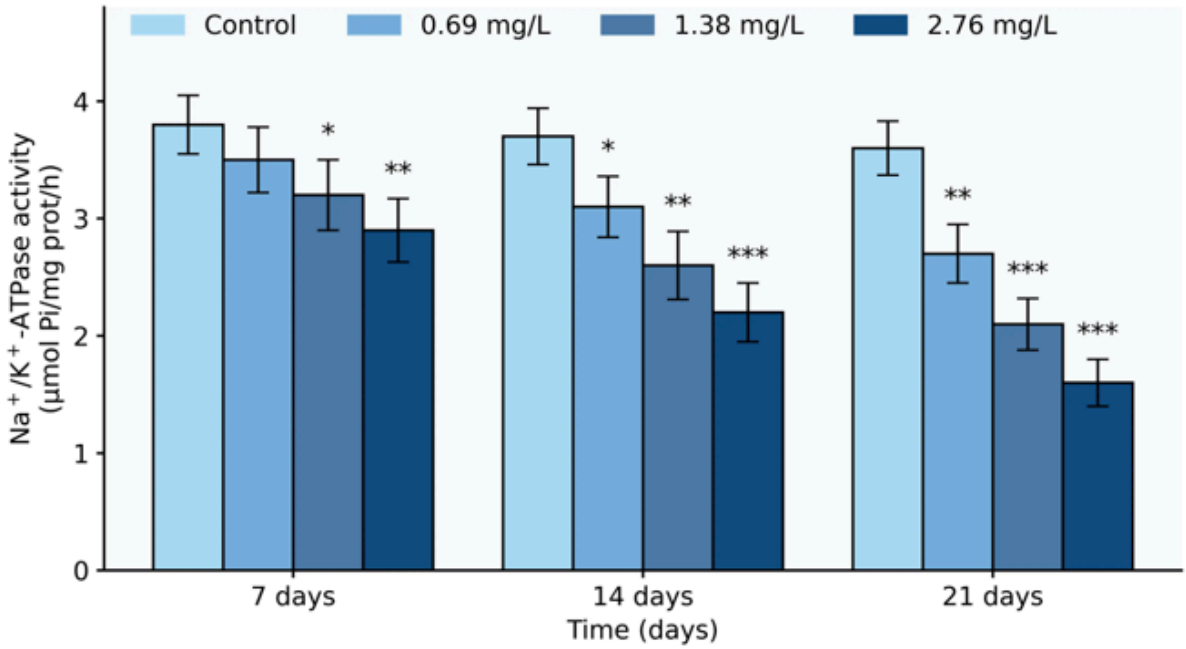


Figure 5

Na^+/K^+-ATPase activity in gill tissue of bighead carp exposed to different SDBS concentrations for 7, 14, and 21 days

Data are presented as mean ± SD (n = 15). *p* < 0.05, **p* < 0.01, ***p* < 0.001 compared to control (two-way ANOVA with Tukey's HSD test).

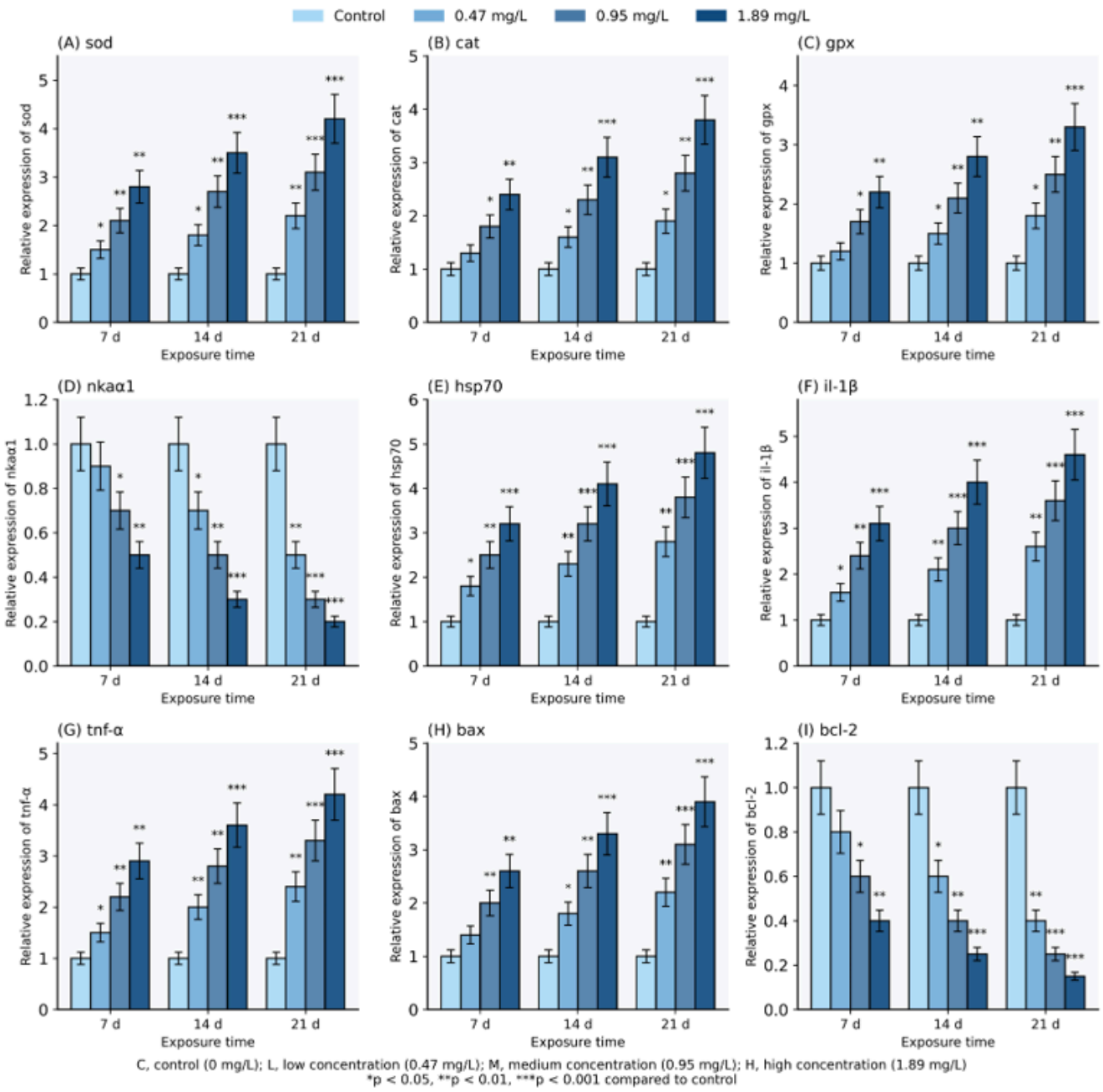


Figure 6

Relative expression levels of target genes in gill tissue of bighead carp exposed to SDBS for 7, 14, and 21 days

Expression of (A) sod, (B) cat, (C) gpx, (D) nkaα1, (E) hsp70, (F) il-1β, (G) tnf-α, (H) bax, (I) bcl-2. Data are presented as mean ± SD (n = 15 per treatment per time point). *p < 0.05, **p < 0.01, ***p < 0.001 compared to control (two-way ANOVA with Tukey's HSD test). C, control (0 mg/L); L, low concentration (0.47 mg/L); M, medium concentration (0.95 mg/L); H, high concentration (1.89 mg/L).

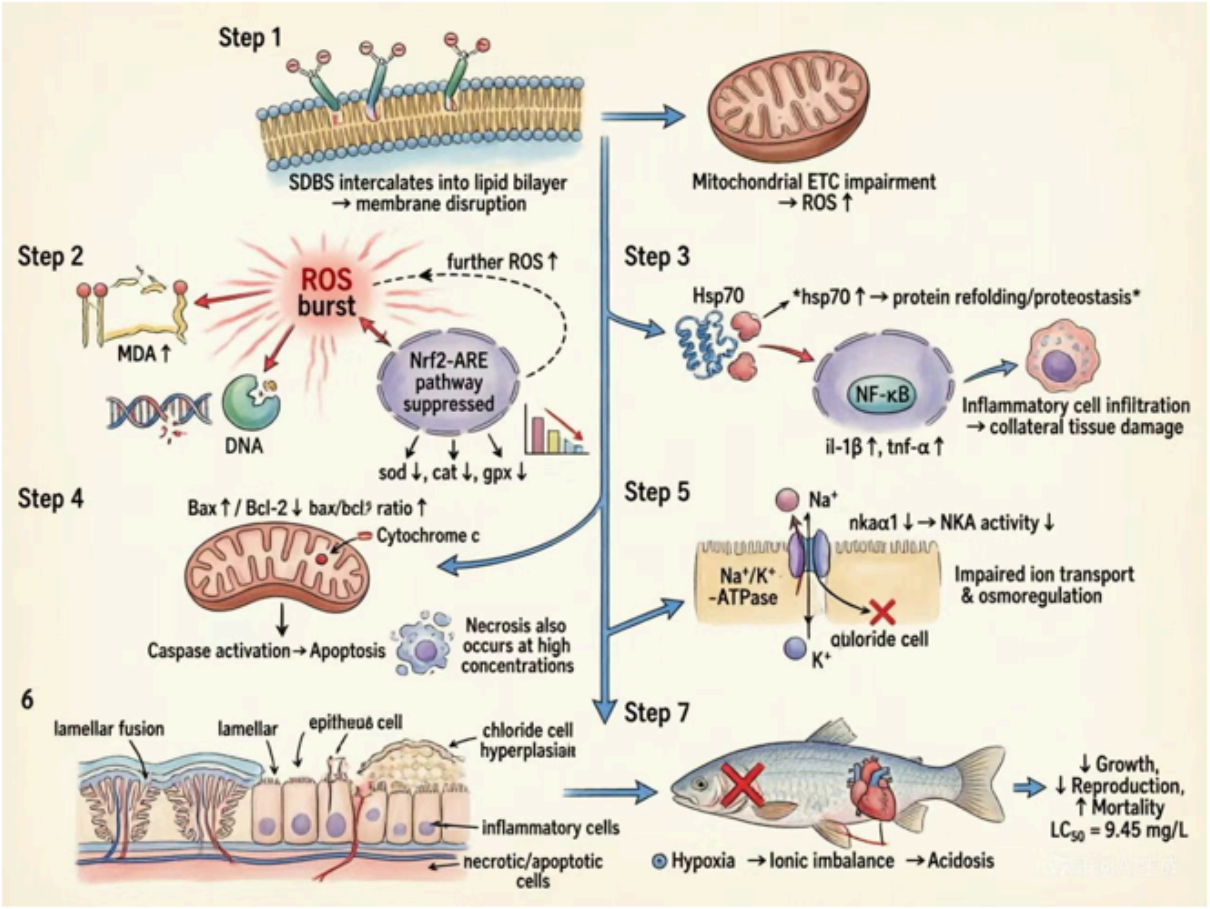


Figure 7

Integrated molecular-to-organismal model of SDBS-induced gill toxicity in bighead carp

Integrated model of SDBS-induced gill toxicity in bighead carp. SDBS disrupts membrane integrity and mitochondrial function, causing ROS overproduction (Step 1). ROS suppress Nrf2-ARE and antioxidant enzymes, while inducing HSP70 and NF-κB-driven inflammation (Steps 2–3). Oxidative stress and TNF-α shift Bax/Bcl-2 ratio, triggering apoptosis (Step 4). SDBS also downregulates NKAα1 and reduces Na^+/K^+-ATPase activity, impairing ion transport (Step 5). These events lead to histopathological lesions (Step 6) and ultimately organ dysfunction, reduced fitness, and mortality (Step 7). Arrows indicate causal links; dashed arrows denote feedback or indirect effects.

Supplementary Files

This is a list of supplementary files associated with this preprint. Click to download.

- Supplementarymaterial.doc